Matrix Metalloproteinase-9 Interplays with the IGFBP2–IGFII Complex to Promote Cell Growth and Motility in Astrocytomas

SANDRINE RORIVE,[1] ALIX BERTON,[1] NICKY D'HAENE,[1] CONSTANTIN NICOLAE TAKACS,[1,4] OLIVIER DEBEIR,[2] CHRISTINE DECAESTECKER,[2,3,5] AND ISABELLE SALMON[1]*

[1]*Department of Pathology, Erasme University Hospital, Université Libre de Bruxelles, Brussels, Belgium*
[2]*Laboratory of Image Synthesis and Analysis (LISA), Faculty of Applied Sciences,*
Université Libre de Bruxelles, Brussels, Belgium
[3]*Laboratory of Toxicology, Institute of Pharmacy, Université Libre de Bruxelles, Brussels, Belgium*
[4]*Yale University, New Haven, Connecticut*
[5]*Fond National de la Recherche Scientifique, Brussels, Belgium*

ABSTRACT
Insulin-like growth factor II (IGFII) acts as a potent mitogen for several tumor types and has been reported to positively influence astrocytoma cell growth and motility. In the central nervous system, IGFII bioavailability is mainly modulated by insulin-like growth factor binding protein 2 (IGFBP2), which sequestrates IGFII and therefore prevents its interaction with the type-1 IGF receptor (IGF-IR). Proteolysis of IGFBP2 is the predominant mechanism recognized to reduce the binding affinity of IGFBP2 for IGFII, thus favoring dissociation of IGFII from the IGFBP2–IGFII complex. It is known that certain proteases involved in astrocytoma malignancy, such as matrix metalloproteinase-7 (MMP-7), plasmin, and cathepsin D, are able to proteolyze IGFBP2 *in vitro*. The present study aims to investigate whether other proteases expressed by astrocytomas, specifically MMP-2, MMP-9, and membrane-type 1 matrix metalloprotease (MT1-MMP), are able to proteolyze the IGFBP2–IGFII complex. Our results show the following: (i) MMP-9 proteolyzes the IGFBP2–IGFII complex *in vitro*, while MMP-2 and MT1-MMP do not; (ii) this MMP-9-induced IGFBP2–IGFII complex proteolysis releases free IGFII, which contributes to enhance the motility and the growth of LN229 astrocytoma cells. Furthermore, this study also highlights that the formation of the IGFBP2–IGFII complex inhibits IGFBP2's cell motility promoting effect by reducing the pool of free IGFBP2. In conclusion, MMP-9-induced IGFBP2 proteolysis may be regarded as an important post-translational event involved in astrocytoma aggressiveness. These new findings support drug targeting of MMP-9 as an interesting approach in the treatment of astrocytoma.   © 2008 Wiley-Liss, Inc.

INTRODUCTION

Aggressiveness of diffuse astrocytomas (WHO grade II–IV) and related mortality are mainly due to two major factors: the rapid growth of the tumor cells and their ability to infiltrate the brain parenchyma (Kleihues and Cavenee, 2000). This migration ability is responsible for astrocytoma cell dissemination from the tumor bulk, which renders impossible the complete resection of the tumor and leads to tumor recurrence and death of the patient (Giese et al., 2003). The interactions between the astrocytoma cells and the extracellular matrix (ECM) components play critical roles in the regulation of cell growth and migration (involving adhesion, motility, and invasion) processes (Friedl et al., 2004). Several proteases, namely plasminogen, activated via the urokinase pathway, cathepsins, and matrix metalloproteinases (MMPs), have been shown to play key roles in these astrocytoma cells–ECM interactions (Bellail et al., 2004; Rao, 2003). The MMPs are expressed as proenzymes that are activated through proteolysis, whereas their activities are inhibited by four endogenous tissue inhibitors (TIMP-1, -2, -3, -4) (Visse and Nagase, 2003). Strong correlations have been reported between increased levels of MMP expression [such as MMP-2, MMP-7, MMP-9, and membrane-type 1 MMP (MT1-MMP)] and astrocytoma malignancy and invasion (Bellail et al., 2004; Nuttall et al., 2003). TIMP-4, widely present in the normal central nervous system (CNS) (Crocker et al., 2004), has been reported to be overexpressed in indolent noninvasive pilocytic astrocytomas (WHO grade I) as compared with diffuse astrocytomas (WHO grade II–IV) (Rorive et al., 2006). TIMP-4 is also known to reduce the invasive ability of astrocytoma cells *in vitro* (Groft et al., 2001). In contrast, TIMP-1 is not observed in normal CNS, but its expression increases dramatically with astrocytoma malignancy (Groft et al., 2001; Lampert et al., 1998; Nakano et al., 1995). While the ECM substrates of the MMPs have been largely well

characterized, identification and study of nonmatrix MMP substrates (such as growth factors and nonmatrix growth factor binding proteins) may provide further valuable insights into the mechanisms of tumor cell proliferation and migration. Knowing the biologic consequences of the MMP-mediated cleavage of these non-ECM substrates may reveal new pathways by which MMPs modulate tumor cell growth, motility, and invasion (McCawley and Matrisian, 2001).

In the CNS, insulin-like growth factors (IGFs, including IGFI and IGFII) promote proliferation, survival, and differentiation of normal neuronal and glial cells, as well as myelination (Baserga et al., 1999; Leventhal et al., 1999; Zeger et al., 2007). Increased expressions of IGFI, IGFII, and the type-1 IGF receptor (IGF-IR) have been documented in many human malignancies, including astrocytomas (Antoniades et al., 1992). Acting as potent mitogens for several tumor cell types, IGFs have been reported to positively influence astrocytoma cell growth and motility *in vitro* (Brockmann et al., 2003; Morford et al., 1997). Six specific binding proteins, i.e., the insulin-like growth factor binding proteins (IGFBP-1, -2, -3, -4, -5, -6), modulate the biologic actions and the bioavailability of the IGFs in either a positive or negative way depending on tissue types and physiologic/pathologic status (Rajaram et al., 1997). This modulation occurs as the IGFBPs sequester the IGFs: the latter thus become unable to bind to their receptor IGF-IR (Firth and Baxter, 2002). Various mechanisms are invoked to explain the release of IGFs from IGFBPs; among them, the proteolytic cleavage of IGFBPs has gained wide acceptance of being the predominant one (Bunn and Fowlkes, 2003). IGFBP2 is widely expressed in the CNS, notably in astrocytic cells (Chesik et al., 2004), and has a higher binding affinity for IGFII than for IGFI (Rajaram et al., 1997). Although IGFBP2 was classically considered as a growth inhibitor, its overexpression is observed in high-grade astrocytomas as compared with low-grade astrocytomas and associated with poor patient survival (Rorive et al., 2006; Sallinen et al., 2000). Actually, IGF-independent effects of IGFBP2 have been described (Hoeflich et al., 2001), and recently, Wang et al. (2006) showed that IGFBP2 positively modulates astrocytoma cell migration through interaction between its Arg–Gly–Asp (RGD) domain and the integrin α5 subunit.

To the best of our knowledge, among the most relevant proteases involved in astrocytoma aggressiveness (Bellail et al., 2004; Rao, 2003), only MMP-7, plasmin, and cathepsin D have so far been reported to cleave IGFBP2 *in vitro* (Claussen et al., 1997; Menouny et al., 1997; Nakamura et al., 2005). We thus hypothesized that MMP-2, MMP-9, and MT1-MMP could also act as IGFBP2 proteinases, resulting in cleavage of the IGFBP2–IGFII complex followed by extracellular release of free IGFII with positive biologic effects on cell growth and migration. The present study aims to test these hypotheses and shows the following: (i) MMP-9 proteolyzes the IGFBP2–IGFII complex *in vitro*, while MMP-2 and MT1-MMP do not; (ii) this proteolysis releases free

IGFII, which contributes to enhance the motility and the growth of LN229 astrocytoma cells.

MATERIALS AND METHODS
Proteins and Reagents

Recombinant human IGFII, IGFBP2, and TIMP-4 were purchased from R&D Systems (Abington, UK). Human-purified pro-gelatinases A (proMMP-2) and B (proMMP-9) and human recombinant MT1-MMP catalytic domain were purchased from Oncogene Research Products (Cambridge, MA). 4-Aminophenylmercuric acetate (APMA) and phorbol 12-myristate 13-acetate (PMA) were purchased from Sigma (St Louis, USA).

Cell Culture

Human LN229 high-grade astrocytoma cells (ATCC number CRL-2611) were grown at 37°C in a 5% CO_2 humidified atmosphere in Dubelcco's Modified Eagle's Medium (DMEM) supplemented with 0.15% $NaHCO_3$, 5% fetal bovine serum (FBS), penicillin G (100 U/mL), streptomycin-sulfate (100 μg/mL), and amphotericin B (250 ng/mL). For the preparation of cell lysates and conditioned media (CM), 3×10^4 LN229 cells were seeded into 35 mm petri Falcon dishes in 3 mL complete medium. The next day, the cells were washed twice with PBS and incubated in 1 mL fresh serum-free medium in the presence or absence of PMA (100 nM). CM was collected after 24, 48 and 72 h, respectively, centrifuged at 10,000g for 10 min and stored at −20°C. The cells were washed twice with ice-cold PBS and lysed at 4°C for 30 min with 500 μL of ice-cold lysis buffer (50 mM Tris–HCL pH 7.6, 150 mM NaCl, 1% NP-40, 1% sodium deoxycholate, 0.1% sodium dodecyl sulphate, 1 mM Na_3VO_4, 1 mM NaF) supplemented with protease inhibitors (Protease Inhibitor Cocktail, Roche Diagnostics). The lysates were centrifuged at 14,000g for 30 min at 4°C, and their protein concentration was determined by using the Bio-Rad Dc protein assay (Hercules, CA).

Enzyme Cleavage Assay

Purified proMMP-2 and proMMP-9 were activated with APMA (1 mM) in an activating buffer [Tris–HCL 50 mM, NaCl 150 mM, $CaCl_2$ 5 mM, pH 7.5] for 2 h at 37°C. IGFBP2 (50 ng) and IGFII [molar ratio (1:5)] were preincubated in an assay buffer [Hepes 100 mM, 44 mM sodium phosphate, 0.1% Triton X-100, 0.1% BSA, pH 7.4] for 1 h at 37°C (Supp. Info. Fig. 1). The IGFBP2–IGFII complex was then exposed to active MMP-2, MMP-9, or to MT1-MMP catalytic domain in the same assay buffer for the times specified in figure legend [substrate:enzyme molar ratio (S:E) ranging from (5:1) to (1:5)]. TIMP-4 (10 μg/mL) was preincubated with active MMP-9 for 1 h prior to addition of the IGFBP2–IGFII complex. After incubation, noncleaved IGFBP2–IGFII

complex was crosslinked with 1.25 mM of BS^3 for 30 min. Excess of BS^3 was blocked with 50 mM Tris–HCL. The reactions were stopped by addition of sample buffer, boiled, and resolved by 15% SDS-PAGE under reducing conditions. In all experiments, both MMP-2 and MMP-9 activations and activities were confirmed by gelatin zymography (GZ).

Immunoblotting

IGFBP2, IGFII, and crosslinked IGFBP2–IGFII complex aliquots were subjected to SDS-PAGE using 15% gels, and transferred to Hybond^{TM}-c Extra nitrocellulose membrane (Amersham, Amersham, UK). Nonspecific binding sites were blocked for 2 h with TBS containing 2% nonfat milk powder, 1% BSA, and 0.05% Tween 20 at room temperature (RT). The membrane was incubated for 2 h in a solution containing goat polyclonal anti-human antibodies (Abs) against IGFBP2 (1:500; sc-6001; Santa Cruz Biotechnology, Santa Cruz, CA) or IGFII (1:1,000; R&D Systems, Abington, UK) at RT and then incubated for 1 h with horseradish peroxydase-conjugated rabbit antigoat antibody (1:50,000; Sigma). For LN229 cells characterization (both under basal condition and after PMA treatment), 45 μg of protein of lysates and LN229 CM (containing the same amount of protein) were run on 15% gels and transferred to membranes. After blocking of nonspecific binding sites, membranes were incubated for 2 h at RT with the relevant primary antibody, i.e. goat polyclonal Abs against human IGFBP2 or IGFII or rabbit polyclonal Abs against human TIMP-4 (1:1,000; AB19168; Chemicon, Temecula, USA) or IGF-IRβ [1:200; sc-713 (C-20); Santa Cruz Biotechnology, Santa Cruz, CA]. Mouse monoclonal Ab against Lamin A/C (1:500; sc-7292; Santa Cruz Biotechnology, Santa Cruz, CA) was used as loading control. The membranes were then incubated for 1 h with the corresponding horseradish peroxydase-conjugated secondary antibody (1:50,000; Sigma). Reactive proteins were detected with the Western lightning^{TM} chemiluminescence reagent (PerkinElmer LAS, Boston, USA).

Gelatin and Casein Zymography Assays

Presence and activity of gelatinases (MMP-2 and MMP-9) and of MMP-7 in LN229 cell lysates and CM (both under basal condition and after PMA treatment) were assayed by substrate gel electrophoresis (zymography) using, respectively, an 8% polyacrylamide gel copolymerized with 0.05% gelatin (Sigma) and a 10% polyacrylamide gel copolymerized with 0.05% casein (Sigma). The gels were run using a vertical gel electrophoresis apparatus at 15 mA into the resolving gel and at 25 mA into the separating gel. The gels were then washed twice in 2.5% Triton X100 and incubated overnight in (50 mM Tris–HCL, 5 mM CaCl$_2$, 0.02% NaN$_3$, 1% Triton X100, 1 μM ZnCl$_2$, pH 7.5) at 37°C. The gels were then stained with Coomassie blue and destained in 7% acetic acid and 20% isopropanol. Purified human proMMP-2 and proMMP-9 were used as positive controls.

Detection of IGFBP2 Proteolysis in LN229 Astrocytoma CM

Equal amount of LN229 CM samples collected after 72 h of cell treatment in the presence of PMA (100 nM) were left untreated or incubated with APMA (1 mM) at 37°C for 18 h. To avoid dilution biases due to addition of APMA in the APMA-treated LN229 CM, the same amount of PBS was added in the APMA-untreated one. Forty microliters of each sample was submitted to gelatin zymography (GZ) and immunoblotting (WB) to detect and quantify changes in MMP-9 activity and in IGFBP2 amount, respectively. Equal amount of untreated LN229 CM were used as control. The resulting immunoblot bands were scanned and the pixel densities evaluated with the Image J software. The presence of IGFBP2 proteolysis was determined by immunoblotting with an anti-IGFBP2 mAb to reveal a decrease of the 36 kDa band size in the LN229 CM samples treated with PMA alone or with PMA and APMA, as compared with the untreated one.

Phosphorylation of IGF-IR

Subconfluent LN229 cells were cultured in serum-free medium for 24 h and then pulsed 5 min with 10 or 100 ng/mL of IGFII. After the stimulation with IGFII, cells were washed twice with ice-cold PBS and lysed at 4°C for 30 min with 500 μL of lysis buffer [20 mM Tris–HCL (pH 7.6), 150 mM NaCl, 1 mM MgCl$_2$, 1% NP40, 10% glycerol, 8 μL of complete protease inhibitor mixture (1 tablet/mL H$_2$O), 1 mM sodium orthovanadate and 10 mM NaF]. The lysates were centrifuged at 14,000g for 30 min at 4°C, and their protein concentration was determined by using the Bio-Rad Dc protein assay (Hercules, CA). Five hundred micrograms of protein of each lysate was immunoprecipitated for 2 h at RT with 3 μg of antiphosphotyrosine mAb (clone 4G10; Upstate Biotechnology, Lake Placid, NY), followed by 2 h of incubation with 50 μL of protein G-Sepharose (Zymed, S. San Francisco, USA). The immunoprecipitates were washed twice with ice-cold lysis buffer. The beads were then resuspended in 50 μL Laemmli sample buffer, boiled for 10 min, and centrifuged at 14,000g for 5 min. The supernatants were fractionated by 7% SDS-PAGE under reducing conditions. Phosphorylated IGF-IR was detected with a rabbit anti-IGF-IRβ polyclonal antibody [1:200; sc-713 (C-20); Santa Cruz Biotechnology, Santa Cruz, CA]. Total level of IGF-IR was detected on hundred micrograms of each lysate resolved by 4–20% Precise Protein Gels (Thermo Fisher Scientific) and immunoblotted with the anti-IGF-IRβ polyclonal antibody. The monoclonal anti-Lamin A/C mAb was used as loading control.

MTT Assay

LN229 cells (2×10^4) were seeded into 96-well plates in complete growth medium. After 24 h, this medium was removed and 100 μL of DMEM containing 1% FBS were added. The adherent cells were pulsed with 10 or 100 ng/mL of IGFII, 514 ng/mL of IGFBP2, the IGFBP2–IGFII complex previously prepared, and MMP-9. The IGFBP2–IGFII complex and MMP-9 were stoechiometrically [1:1] preincubated for 1 h at 37°C. Before exposure of the cells to APMA-activated MMP-9, APMA was removed using desalting columns (Pierce Biotechnology, Rockford, USA). To avoid biases due to persisting traces of APMA in the MMP-9 conditions, the same amount of desalted APMA solution was added to the control and IGFBP2–IGFII complex conditions, when both were compared with MMP-9 cell treatment. In some experiments, LN229 cells were preincubated for 1 h with the anti-IGF-IR antibody (1 μg/mL; clone αIR3, IgG1, Oncogene Research Products, Cambridge, MA) or its respective mouse isotype IgG1, and then stimulated by 100 ng/mL of IGFII. After treatment for 0, 3, or 6 days, the cells were incubated in 100 μL of DMEM medium containing 0.5 mg/mL (3-(4, 5-dimethylthiazolyl-2)-2,5-diphenyltetrazolium bromide (MTT) for 3 h. The MTT solution was then discarded and the formazan produced by the living cells solubilized in 1 mL HCL 1 M/isopropanol [1:24]. The absorbance was read at 570 nm using the BIO-RAD microplate reader (Model 688). Each experimental condition was run in at least quintuplicate.

Video Microscopy Cell Motility Assay

LN229 cells (2×10^5) were seeded into 25-cm^2 flasks in a complete growth medium. After 48 h, the medium was removed and 7 mL of DMEM containing 1% FBS were added. The cells were pulsed, respectively, with 10 or 100 ng/mL of IGFII, 514 ng/mL of IGFBP2, the IGFBP2–IGFII complex previously prepared, and MMP-9. The IGFBP2–IGFII complex and MMP-9 were stoechiometrically [1:1] preincubated for 1 h at 37°C. Before cell exposition to APMA-activated MMP-9, APMA was removed by means of a desalting column. The motility assay was performed as previously described (Rorive et al., 2001). Briefly, the cells were maintained at 37°C and observed by phase-contrast microscopy (Olympus, model IX50, magnification ratio 10:1). Phase-contrast micrographs were automatically recorded every 4 min during 48 h with CCD cameras (Hitachi Denshi, model KP-M1E/K-S10). Cell motility was analyzed using a recently improved cell-tracking algorithm, which is able to reconstruct the individual trajectories of the observed cells (Debeir et al., 2005). To evaluate the amplitude of the cell movements, we used the maximal diameter of each cell trajectory, i.e. the maximum distance between any two points constituting the trajectory (Debeir et al., 2005). Each condition was run in three independent experiments.

Statistic Analyses

The Kruskal–Wallis test was used to compare independent groups of numeric data. When this multigroup test was significant, posthoc tests (Dunn procedure) were used to compare the group pairs of interest, thus avoiding multiple comparison effects.

RESULTS
MMP-9 Proteolyzes the IGFBP2–IGFII Complex

In this study, we tested the ability of MMP-2, MMP-9, and MT1-MMP to proteolyze IGFBP2 and the IGFBP2–IGFII complex. Stable and reproducible IGFBP2–IGFII complex was identified by immunoblotting [Fig. 1A, Lane 2; see Supporting Information Fig. 1 for more details] prior to exposure to active MMPs. Immunoblotting revealed that neither MMP-2 nor the MT1-MMP catalytic domain were able to proteolyze the IGFBP2–IGFII complex (Fig. 1A, Lanes 3–5 and 9–11). In contrast, the IGFBP2–IGFII complex was stoichiometrically [1:1] cleaved by MMP-9 (Fig. 1A, Lanes 6–8). The activity of the MT1-MMP catalytic domain (exposed to the IGFBP2–IGFII complex) was confirmed by evidencing its proteolytic action on free IGFBP2 (tested in the same experiment) (Fig. 1C). Both MMP-2 and MMP-9 activations and activities were confirmed by gelatin zymography (Fig. 1D). MMP-9 cleaved the IGFBP2–IGFII complex in a time-dependent manner with a complete proteolysis after 6 h (Fig. 2A,B). IGFBP2 was proteolyzed, and in parallel, a release of IGFII was observed after 3 h (Fig. 2A, Lane 5). TIMP-4, reported to be negatively associated with astrocytoma malignancy (Rorive et al., 2006) and able to reduce glioblastoma invasion *in vitro* (Groft et al., 2001), inhibited partially this proteolytic activity of MMP-9 (Fig. 2B, Lane 6).

MMP-9 Secreted by LN229 Astrocytoma Cells Induces IGFBP2 Proteolysis in Conditioned Media

Phorbol 12-myristate 13-acetate (PMA) was previously described to induce MMP-9 expression in normal and tumoral astrocytes, through activation of the Protein Kinase C pathway (Arai et al., 2003; Woo et al., 2005). We performed gelatin zymography (GZ) to determine whether PMA increases the MMP-9 expression and/or activity in LN229 astrocytoma cells. As shown in Fig. 3A, exposure to PMA (100 nM for 72 h) resulted in a dramatic secretion of the 92 kDa proMMP-9 in LN229 CM, whereas the secretion of the 72 kDa proMMP-2 was not enhanced and even slightly decreased. In addition, a 125 kDa gelatinolytic band, already observed in LN229 untreated CM, appeared duplicated after PMA stimulation, suggesting activation. This 125 kDa band, also detected by immunoblotting with an anti-MMP-9 mAb (see Supp. Info. Fig. 2), was previously reported to be a complex of proMMP-9 with lipocalin (Yan et al., 2001). No MMP-7 activity was observed in LN229 cell lysates
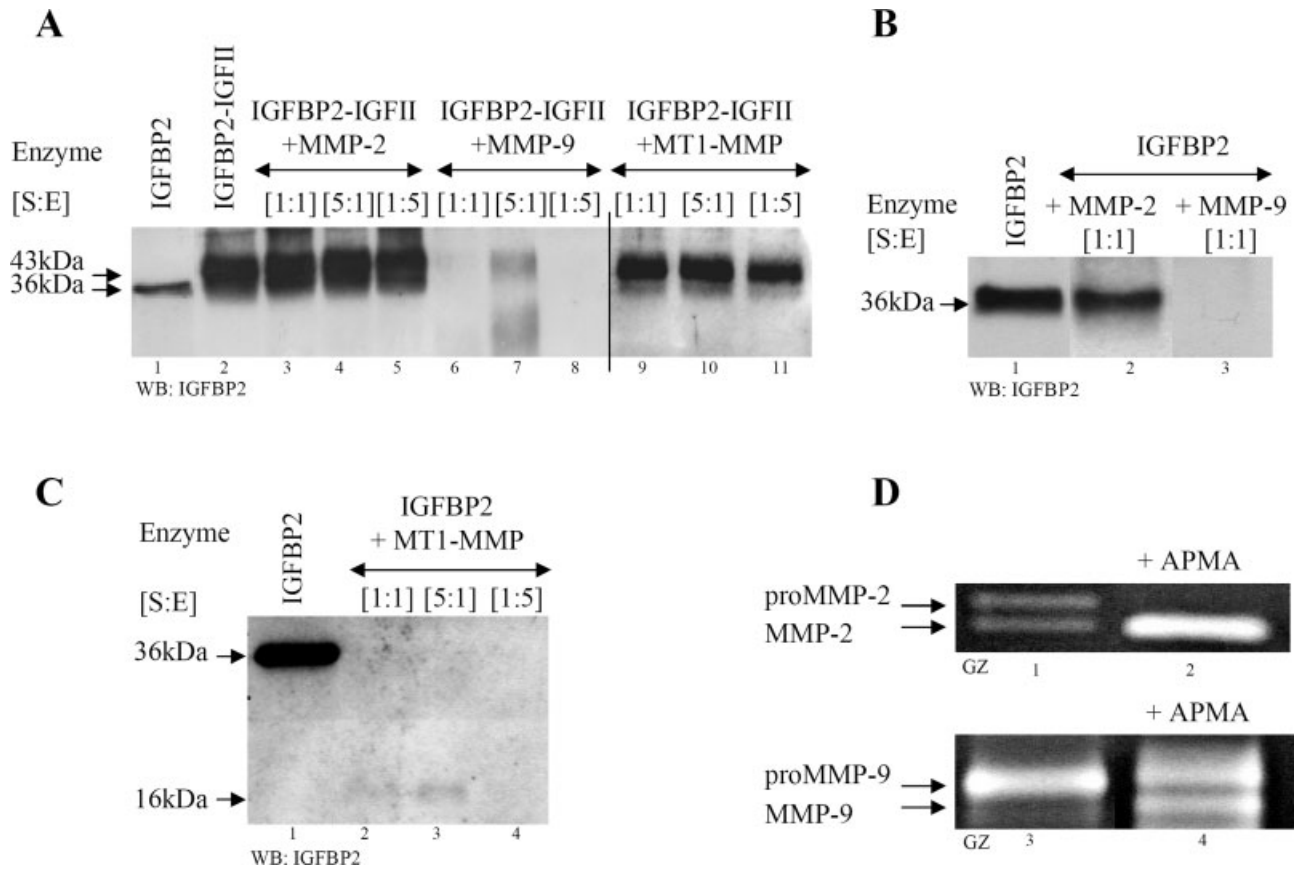
Fig. 1. Proteolytic activities of MMP-2, MMP-9, and MT1-MMP on free IGFBP2 and the IGFBP2–IGFII complex. (**A**) Human recombinant IGFBP2 and human recombinant IGFII proteins [molar ratio (1:5)] were preincubated in an assay buffer to form the IGFBP2–IGFII complex (IGFBP2–IGFII). Immunoblotting with an anti-IGFBP2 mAb (WB:IGFBP2) reveals IGFBP2 and the stabilized IGFBP2–IGFII complex with respective molecular masses of 36 and 43 kDa, and the presence or absence of proteolytic abilities of active MMP-2, MMP-9, and MT1-MMP (separate experiment for this latter) on the IGFBP2–IGFII complex [substrate/enzyme molar ratio (S:E) = (1:1), (5:1), (1:5)]. (**B,C**) Immunoblottings with an anti-IGFBP2 mAb show the presence or absence of proteolytic abilities of active MMP-2 and MMP-9 [B, (S:E) = (1:1)] and of the MT1-MMP catalytic domain [C, (S:E) = (1:1), (5:1), (1:5)] on free IGFBP2. (**D**) Gelatin zymograms (GZ) characterize activations and activities of both the MMP-2 and the MMP-9 used in (A) and (B) experiments after being exposed to APMA 1 mM. (A–C) All experiments were carried out for 20 h at 37°C.

and CM under either basal status or PMA stimulation (data not shown). Figure 3B shows that exposure to PMA did not change the levels of IGFBP2, TIMP-4, and IGF-IR expression in LN229 cell lysates (Fig. 3B, Lanes 1 and 2) and did not induce TIMP-4 secretion in CM (Fig. 3B, Lanes 3 and 4). However, CM from PMA-treated cells contained lower levels of IGFBP2 than the CM from untreated cells (Fig. 3B, Lane 4 *vs.* 3). Densitometric measurements of the IGFBP2 band intensities confirmed that the IGFBP2 level was reduced by more than 30% in the media of PMA-stimulated cells as compared with media from unstimulated ones (34–59% in the five different experiments carried out). The 125 kDa proMMP-9, once activated, may thus at least partially be responsible for the decreased level of IGFBP2 noted in Fig. 3B (Lane 4) and Fig. 3D (Lane 2).

We then investigated whether activation of the 92 kDa proMMP-9 secreted by LN229 cells after PMA stimulation increased the amount of IGFBP2 proteolysis in LN229 CM. For this purpose, LN229 CM collected after 72 h of PMA stimulation was incubated with APMA (1 mM) for 18 h, and then submitted to gelatin zymography (GZ) and immunoblotting with an anti-IGFBP2 mAb (WB:IGFBP2). Gelatin zymography confirmed an increase of the active 82 kDa MMP-9 band after APMA treatment (Fig. 3C, Lane 3); simultaneously, the IGFBP2 band intensity decreased (Fig. 3D, Lane 3).

IGFII, IGFBP2 and the Proteolysis Products of the IGFBP2–IGFII Complex Stimulate LN229 Cell Motility

Before carrying out the different cell assays, we showed that LN229 cells express IGF-IR, which becomes autophosphorylated in response to IGFII treatment in a dose-dependent manner (see Fig. 4).

Videomicroscopy and adapted cell tracking algorithms allowed us to quantify LN229 cell motility as illustrated in Figs. 5 and 6. While Fig. 5 shows the cell trajectories covered by LN229 cells over 12 h in a representative experiment of each condition, Fig. 6 displays the extracted quantitative results. As compared with control, no statistic variation in cell motility was observed
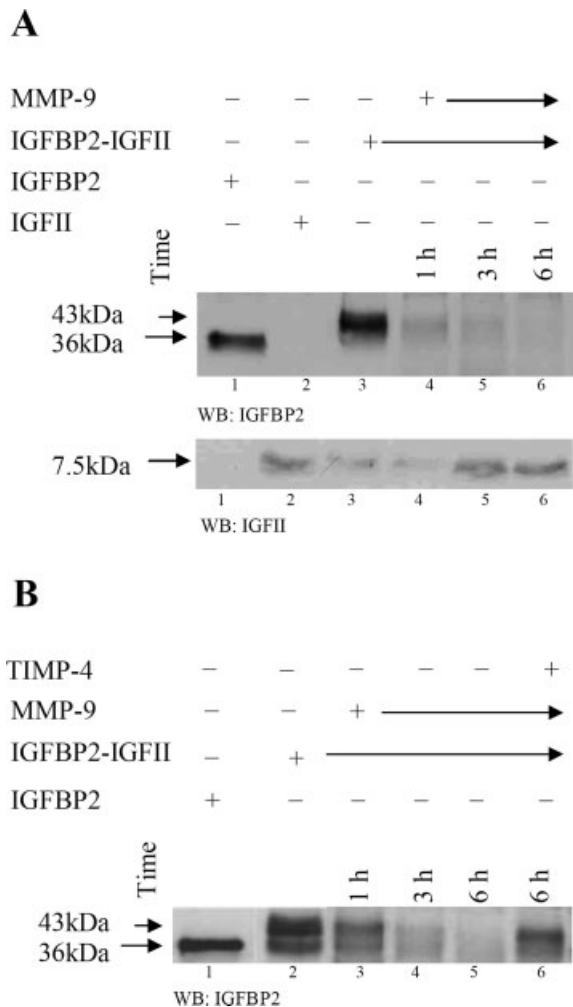
A

WB: IGFBP2

WB: IGFII

B

WB: IGFBP2

Fig. 2. Characterization of the MMP-9 proteolytic activity on the IGFBP2–IGFII complex. (**A**) The time-course of the MMP-9-induced proteolysis of the IGFBP2–IGFII complex using immunoblotting with an anti-IGFBP2 mAb (WB:IGFBP2) and an anti-IGFII mAb (WB:IGFII) on the same membrane [substrate/enzyme molar ratio (S:E) = (1:1)]. (**B**) Immunoblotting with an anti-IGFBP2 mAb in which the IGFBP2–IGFII complex was exposed to active MMP-9 [(S:E) = (1:1)] alone or in the presence of excess of TIMP-4 for 6 h at 37°C (Lane 6). The 43 kDa band corresponds to the IGFBP2–IGFII complex, while the 36 kDa band indicates free IGFBP2.

when LN229 cells were exposed to 10 ng/mL of IGFII at different time steps (12 and 24 h), whereas their trajectory diameters dramatically increased when pulsed with 100 ng/mL of IGFII for 24 h ($P < 0.001$; Fig. 6A). This positive motogenic effect was already present after 12 h of cell treatment ($P < 0.01$; Fig. 6B). The dose-dependent response of LN229 cell motility to IGFII is similar to the phosphorylation response of IGF-IR mainly observed with 100 ng of IGFII in our model (see Fig. 4). Figure 6B also shows that IGFBP2 significantly enhanced LN229 cell motility as compared with control ($P < 0.01$), whereas both IGFII and IGFBP2 positive motogenic effects were completely inhibited when these proteins formed a complex. To determine the cell motility response to the MMP-9 induced proteolysis of the IGFBP2–IGFII complex, LN229 cells were treated with

MMP-9, the IGFBP2–IGFII complex, or both (Fig. 6C). We observed a positive action of MMP-9 on the motility of LN229 cells as compared with control ($P < 0.05$). In addition, when LN229 cells were treated with the IGFBP2–IGFII complex in the presence of MMP-9, the cell motility dramatically increased ($P < 0.001$).

IGFII, the IGFBP2–IGFII Complex and Its Proteolysis Products Modulate LN229 Cell Growth

The IGFII influence on LN229 cell growth was determined by carrying out MTT assays on LN229 cells treated with 10 or 100 ng/ml of IGFII for 6 days (Fig. 7A). Only 100 ng/ml of IGFII was able to significantly increase LN229 cell growth ($P < 0.05$). As already noted for cell motility, this dose-dependent response is similar to the phosphorylation response of IGF-IR (see Fig. 4). As shown in Fig. 7B, the IGFII-induced stimulation of LN229 cell growth appeared as a late event, which was not yet present after 3 days of cell treatment. Confirming the specificity of this result, pretreating LN229 cells with the anti-IGF-IR α-IR3 (1 µg/mL) totally abolished this late IGFII-induced stimulation of LN229 cell growth ($P < 0.01$), whereas the specific mouse isotype was devoid of effect (data not shown). Addition of IGFBP2 alone did not alter LN229 cell growth. In contrast, formation of the IGFBP2–IGFII complex counteracted the positive influence of IGFII on LN229 cell growth and even inhibited LN229 cell growth as compared with control ($P < 0.05$; Fig. 7B). To evaluate the cell growth response to MMP-9-induced proteolysis of the IGFBP2–IGFII complex, LN229 cells were treated with MMP-9, alone or in the presence of the IGFBP2–IGFII complex (Fig. 7C). We first evidenced a positive and significant effect of MMP-9 on LN229 cell growth as compared with control ($P < 0.01$). In contrast to the IGFII-induced effect, the MMP-9 one appeared as an earlier event (i.e. after 3 days), which was maintained after 6 days. Secondly, when LN229 cells were treated with MMP-9 in the presence of the IGFBP2–IGFII complex, the cell growth level significantly increased compared with the IGFBP2–IGFII complex alone, at day 3 and day 6 ($P < 0.01$). To distinguish the effects due to MMP-9 alone from those due to the IGFBP2–IGFII complex proteolysis, we computed and analyzed the increases in cell growth caused by MMP-9 exposure in the absence or presence of the IGFBP2–IGFII complex (see arrows in Fig. 7C). While at day 3, both increases in cell growth were similar, at day 6 they significantly differed ($P < 0.01$) suggesting an additional effect from the MMP-9-induced IGFBP2–IGFII complex proteolysis.

DISCUSSION

During recent years, the knowledge of the relevance of proteases in cancer research has grown considerably. These enzymes, initially viewed as ECM destroyers associated with tumor cell invasion, are now known to
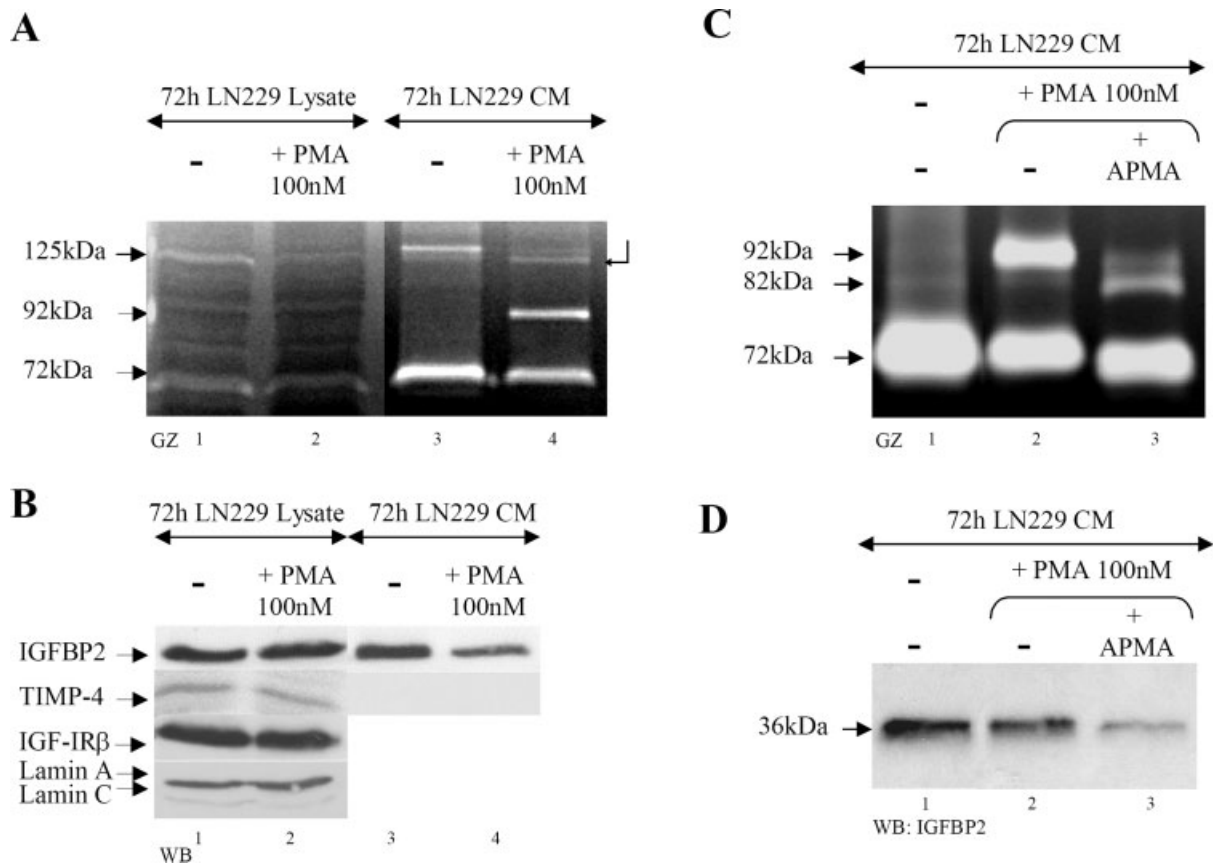
Fig. 3. LN229 is an adequate model to investigate the MMP-9-induced IGFBP2 proteolysis. (**A**) PMA increases proMMP-9 secretion by LN229 cells. LN229 cells were treated in the absence or presence of PMA (100 nM) for 72 h in serum-free media. LN229 lysates and conditioned media (CM) were characterized by gelatin zymography (GZ). Gelatinolytic activities of the 72 kDa proMMP-2 and both the 92 kDa and the 125 kDa proMMP-9 appear as clear bands. The 125 kDa band, which corresponds to the heterodimer of proMMP-9 with lipocalin, is partially activated after PMA treatment (⌐). (**B**) PMA induces IGFBP2 proteolysis in LN229 CM. The LN229 lysates and CM used for the zymography shown in (A) were characterized by immunoblotting (WB) with anti-IGFBP2, -TIMP-4, and -IGF-IRβ mAbs, respectively. The monoclonal anti-Lamin A/C mAb was used as loading control. (**C**) APMA increases MMP-9 activity in LN229 CM. LN229 CM collected after PMA exposure was incubated with APMA (1 mM) for 18 h and characterized by gelatin zymography (GZ). Gelatinolytic activities of the 72 kDa proMMP-2, the 92 kDa proMMP-9, and the 82 kDa active MMP-9 appear as clear bands. (**D**) APMA induces IGFBP2 proteolysis in LN229 CM. The LN229 CM used for the zymography shown in (C) was characterized by immunoblotting with an anti-IGFBP2 mAb. IGFBP2 proteolysis was noted by a decrease of the 36 kDa band size intensity.

play other critical roles in tumor progression, involving cell growth, cell migration, and angiogenesis (Egeblad and Werb, 2002). In the tumoral microenvironment, the ECM is more than a barrier against invasion. It also serves as a reservoir of cell-binding proteins and growth factors that can be released by proteolysis or remodeling processes. Cleavage of some of these proteins may thus generate bioactive fragments, which may be able to signal through interactions with cell surface receptors (DeClerck et al., 2004). In this context, the proteases that target IGFBPs are emerging as key regulators of IGFs actions at the cell surface. IGFBP proteolysis generates fragments that have greatly reduced affinity for IGFs, increasing the concentration of free IGFs at the cell surface and allowing binding and activation of the type-1 IGF receptor (IGF-IR) (Bunn and Fowlkes, 2003). This mechanism is known to occur under physiologic conditions in a variety of biologic fluids and tissues. However, IGFBP proteolysis may be exacerbated in certain pathologic conditions, such as malignancies, in
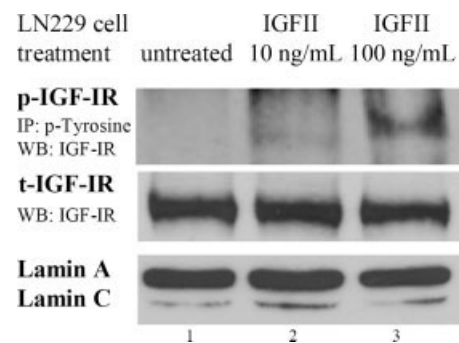

Fig. 4. LN229 cells express IGF-IR, which becomes autophosphorylated in response to IGFII. Subconfluent LN229 cells were pulsed with either 10 ng/mL IGFII or 100 ng/mL IGFII for 5 min at 37°C. Each cell lysate was immunoprecipitated with the antiphosphotyrosine mAb (clone 4G10) and separated by SDS-PAGE. The blotted proteins were detected with an anti-IGF-IR mAb. For each condition tested, the total (t-IGF-IR) and the phosphorylated (p-IGF-IR) IGF-IR levels are shown. The monoclonal anti-Lamin A/C mAb was used as loading control.

CT   **IGFII**

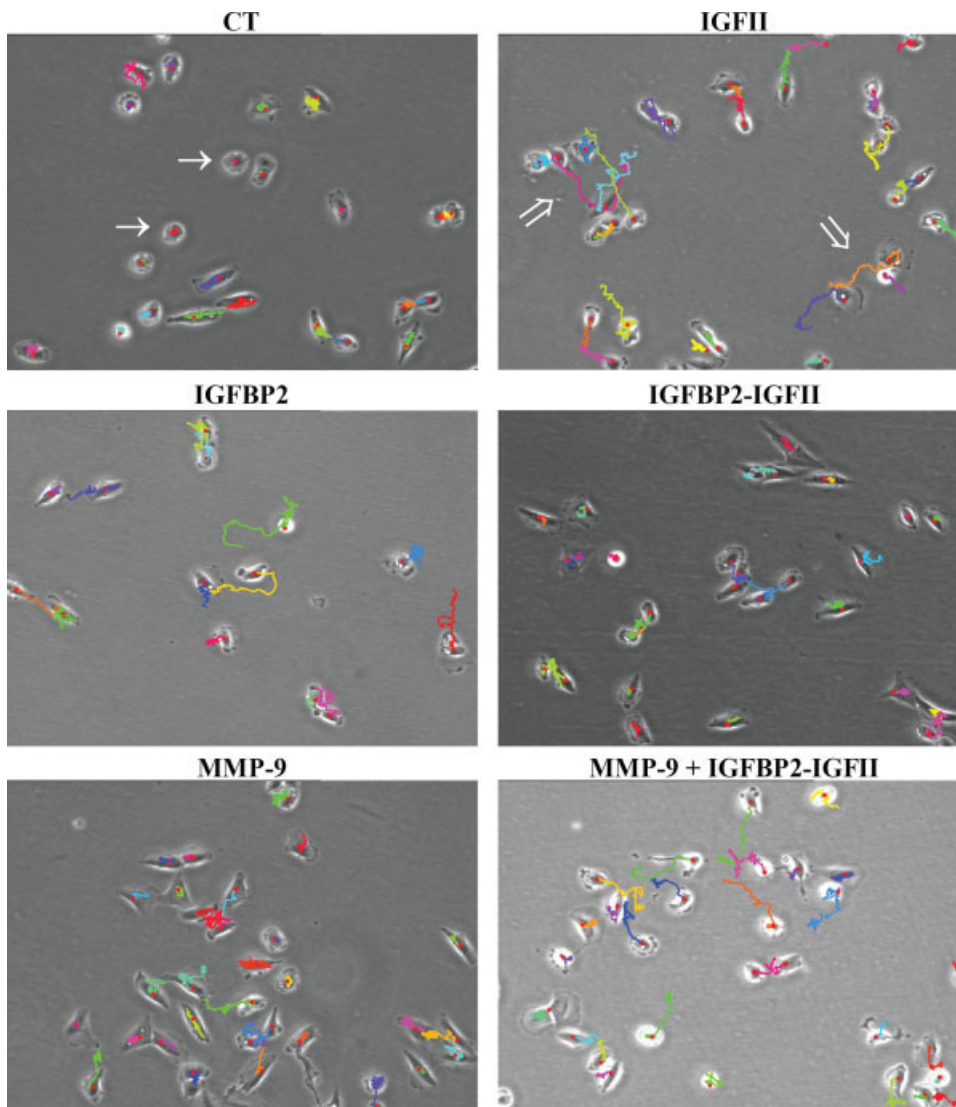**IGFBP2**   **IGFBP2-IGFII**

Fig. 5. Individual cell trajectory reconstruction using phase-contrast video microscopy and automatic cell tracking. Illustration of representative trajectories covered by LN229 cells after 12 h of monitoring in the different experimental conditions. The red points centered on cells locate the beginning of the trajectories. Each trajectory superposed on the first image of the sequence recorded is represented by a color curve ($\Rightarrow$), which is reduced to the initial red point in the case of immotile cells ($\rightarrow$). IGFII added alone or released from the IGFBP2–IGFII complex by MMP-9 (MMP-9 + IGFBP2–IGFII) both increased the amplitude of the cell movements as compared with the CT and IGFBP2–IGFII conditions (for statistical results, see Fig. 6).

MMP-9   **MMP-9 + IGFBP2-IGFII**

which proteases are overexpressed, hypersecreted, and/or excessively activated (Rajaram et al., 1997).

Several proteases are well known for playing a number of critical roles in progression and invasion of the diffuse grade II–IV astrocytomas (Bellail et al., 2004; Giese et al., 2003; Rao, 2003). The most active MMPs involved in these processes are MMP-2, MMP-7, MMP-9, and MT1-MMP (Belien et al., 1999; Nakano et al., 1995; Nuttall et al., 2003). All four MMPs have abilities to proteolyze both ECM- and non-ECM-substrates, thus using different pathways to alter the tumor cell behavior (Imai et al., 1997; Kajita et al., 2001; McCawley and Matrisian, 2001; Yu and Stamenkovic, 2000). MMP-2, MMP-7, and MMP-9 have been previously reported to cleave certain IGFBPs. Both MMP-2 and MMP-9 are able to proteolyze IGFBP1 (Coppock et al., 2004; Manes et al., 1997) and IGFBP3 (Fowlkes et al., 1994; Manes et al., 1999), while only MMP-2 has proteolytic effect on IGFBP5 (Thrailkill et al., 1995). MMP-7 was recently reported to proteolyze all six IGFBPs (Miyamoto et al.,

2004; Nakamura et al., 2005). The present work focuses on the widely expressed IGFBP in the CNS, IGFBP2 (Baserga et al., 1999; Leventhal et al., 1999). We showed for the first time, to the best of our knowledge, that MMP-9 acts as an IGFBP2-proteinase on the IGFBP2–IGFII complex *in vitro* and noted that TIMP-4 inhibits partially this proteolysis. We then noticed the presence of IGFBP2 proteolysis in LN229 astrocytoma cell culture media simultaneously to increase of MMP-9 activation. In contrast, we showed that neither MMP-2 nor MT1-MMP has the ability to proteolyze the IGFBP2–IGFII complex *in vitro*, even when added in excess. This result on MMP-2 contradicts a previous one observed in the late stages of rat osteoblasts differentiation, which showed that the extent of IGFBP2 proteolysis was correlated with increased levels of active MMP-2 (shown by gelatin zymography) in the media conditioned by these cells (Palermo et al., 2004). However, the specificity of this MMP-2 activity was not confirmed, whereas TIMP-1 was able to inhibit IGFBP2 degradation in this model.

While current literature provides compelling evidences for the regulatory role of the IGF system in cell growth and motility (Baserga et al., 1999; Guvakova, 2007; Leventhal et al., 1999), only few data concern IGFII and its involvement in astrocytoma aggressiveness. Several reasons lead us to study IGFII as a ligand to IGF-IR. First, in the CNS, IGFII (in contrast to IGFI) is most highly expressed in non-neuronal tissues such as leptomeninges, parenchymal microvasculature, and myelin sheaths

of axons (Chesik et al., 2007). IGFII was found to colocalize with IGFBP2 in these structures (Chesik et al., 2007), which are well known to provide substrates for astrocytoma cell migration (Bellail et al., 2004). Second, IGFII binds IGFBP2 with higher affinity than IGFI (Rajaram et al., 1997). Finally, IGFII is thought to play crucial roles in the pathogenesis of various human cancers (Toretsky and Helman, 1996), and its gene was recently showed to be overexpressed in a subclass of glioblastoma characterized by poor survival (Soroceanu et al., 2007).

LN229 astrocytoma cells express IGF-IR, which becomes autophosphorylated in response to physiologic doses of IGFII, a *sine qua non* condition to evaluate the biologic impact of IGFII in our model. We showed that IGFII promotes LN229 cell growth and motility. This study is the second one to report a positive involvement of IGFII in astrocytoma cell motility *in vitro* (Brockmann et al., 2003). We thus confirmed that IGFII enhances astrocytoma aggressiveness through notable both growth- and motility-promoting effects.

The colocalization of IGFII and IGFBP2 in brain structures (see above) suggests that IGFBP2 may act as a modulator of IGFII actions in the CNS (Chesik et al., 2007). The effects mediated by the IGFBP2–IGFII complex on the LN229 cells reported in the present study support this hypothesis, and also suggest that this complex acts as a negative modulator of astrocytoma cell growth. In addition, we observed that IGFBP2 alone has no effect on astrocytoma cell growth *in vitro*, whereas it positively affects astrocytoma cell motility. Both results are in agreement with previous studies recently published in literature (Levitt et al., 2005; Wang et al., 2003, 2006). The latter of these studies reported that IGFBP2 promotes astrocytoma cell motility through interaction between the integrin α5 subunit and its RGD domain. Interestingly, we noted that when IGFBP2 bound IGFII in the IGFBP2–IGFII complex, its positive influence on cell motility completely disappeared. This latter result suggests that, in addition to preventing the interaction between IGFII and IGF-IR, the formation of
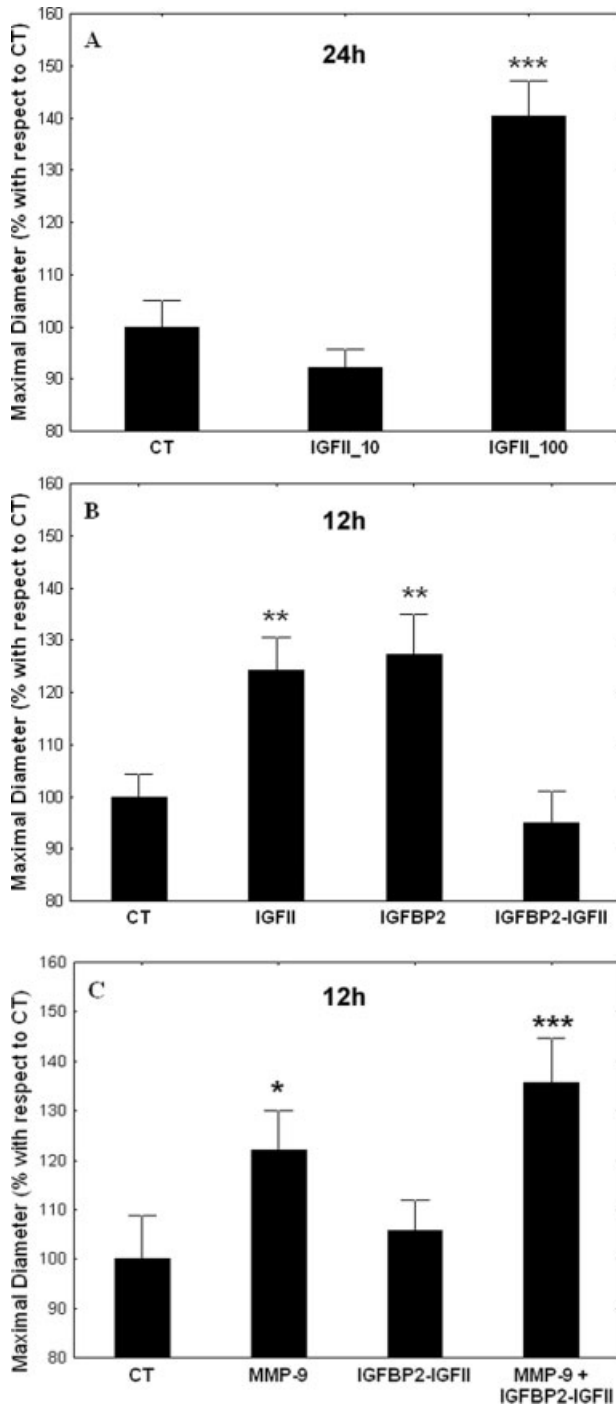

Fig. 6. IGFII, IGFBP2 and the proteolysis products of the IGFBP2–IGFII complex stimulate cell motility. (**A**) IGFII induces a dose-dependent effect on LN229 cell motility. Cells were cultivated in medium with FBS 1% (CT) and exposed to 10 ng/mL (IGFII_10) or 100 ng/mL (IGFII_100) of IGFII for 24 h. (**B**) LN229 cell motility response to IGFII, IGFBP2, and the IGFBP2–IGFII complex. Cells were cultivated in medium with FBS 1% (CT) and exposed to 100 ng/mL of IGFII, 514 ng/mL of IGFBP2, or the IGFBP2–IGFII complex previously formed, for 12 h. (**C**) LN229 cell motility response to the products of the IGFBP2–IGFII complex proteolysis by MMP-9. Cells were cultivated in medium with FBS 1% (CT) and exposed to MMP-9, the IGFBP2–IGFII complex, or to the IGFBP2–IGFII complex in the presence of MMP-9 [1:1], for 12 h. Before cell exposition to APMA-activated MMP-9, APMA was removed using desalting columns. (A–C) Cell motility was quantitatively assessed by the maximal diameter of each cell trajectory. Each condition was run in three independent experiments pooled for statistic analysis. The data are expressed in terms of means ± SE normalized so that the control (CT) mean was set to 100. As compared with CT, only the significant differences (posthoc tests) are indicated as *$P < 0.05$, **$P < 0.01$, and ***$P < 0.001$.

the IGFBP2–IGFII complex may also prevent the interaction between the IGFBP2 RGD domain and the integrin α5 subunit, showed by Wang et al. (2006) as being essential for the IGFBP2-induced cell motility.

Different methodologies are available to investigate how MMP-9 influences cell behavior *in vitro*. In the present study, we directly exposed LN229 cells to exogenous human purified MMP-9, and showed that MMP-9 acts as a stimulator of both astrocytoma cell growth and motility. Similar results were indirectly reported by Lakka et al. (2002), who showed that the downregulation of MMP-9 expression reduced astrocytoma cell growth, motility, and invasion. In addition to direct MMP-9-induced stimulation of cell growth and motility, we showed that the proteolysis of the IGFBP2–IGFII complex by MMP-9 caused a dramatic increase in both cell growth and cell motility, suggesting that MMP-9 and the IGF system may collaborate to promote astrocytoma aggressiveness. We thus provide a new evidence to validate the usefulness of targeting MMP-9 in the treatment of astrocytoma.

To date, MMP inhibitors have shown little clinical benefits when used as monotherapy in patients with advanced disease, whereas novel agents are still tested in trials (Chiappori et al., 2007). Short interfering RNA (siRNA) was recently shown to be an effective method for inhibiting the expression of a specific gene in human cells, and current published data suggest antitumor potential effects of this technique (Tong et al., 2005). Indeed, a siRNA sequence of human *MMP-9* was shown to inhibit medulloblastoma cell growth and invasion both *in vitro* and *in vivo* (Rao et al., 2007). Furthermore, simultaneous downregulation of uPAR and MMP-9 expression by means of RNA interference dramatically reduced glioblastoma growth, invasion, and angiogenesis in both *in vitro* and *in vivo* models (Lakka et al., 2005). The IGF system and its actors (including the IGFs, IGF-IR, and their downstream signaling effectors) were also proposed as promising targets for therapeutic approaches in malignant astrocytomas (Andrews et al., 2001). Numerous molecular antisense strategies targeting these agents are now tested in many clinical trials for the search of alternative treatment in human malignant astrocytoma (Trojan et al., 2007).

In summary, this work suggests that MMP-9-induced IGFBP2 proteolysis is an important post-translational event that contributes to increase IGFII bioavailability and astrocytoma aggressiveness. These new findings
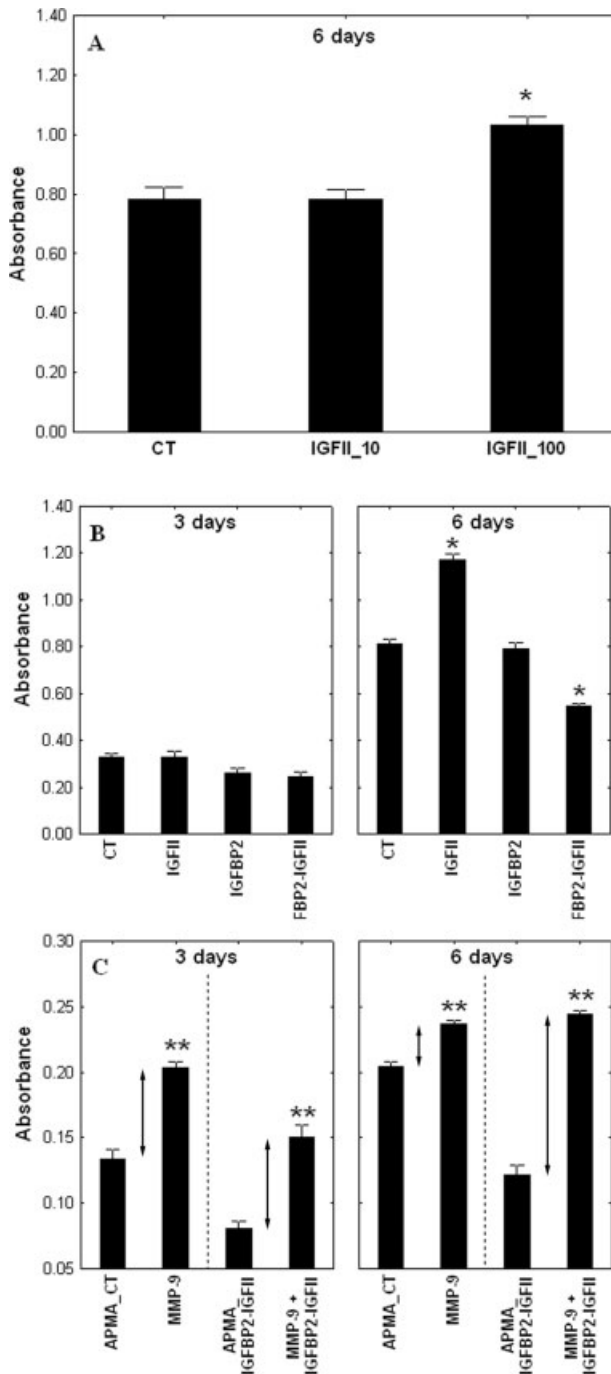

Fig. 7. IGFII, the IGFBP2–IGFII complex and its proteolysis products modulate cell growth. (**A**) IGFII induces a dose-dependent effect on LN229 cell growth. Cells were plated in equal amount, cultivated in medium with FBS 1% (CT), and exposed to 10 ng/mL (IGFII_10) or 100 ng/mL (IGFII_100) of IGFII. MTT conversion was measured after 6 days. The experiments were carried out in sextuples. (**B**) LN229 cell growth response to IGFII, IGFBP2, and the IGFBP2–IGFII complex. Cells were plated in equal amount, cultivated in medium with FBS 1% (CT), and exposed to 100 ng/mL of IGFII, 514 ng/mL of IGFBP2, or the IGFBP2–IGFII complex previously formed. (**C**) LN229 cell growth response to the products of the IGFBP2–IGFII complex proteolysis by MMP-9. Cells were plated in equal amount, cultivated in medium with FBS 1%, and exposed to MMP-9, the IGFBP2–IGFII complex, or to the IGFBP2–IGFII complex in the presence of MMP-9 [1:1]. To avoid biases due to persisting traces of APMA in the MMP-9 conditions (see Materials and Methods), the same amount of desalted APMA solution was added to the control (APMA_CT) and IGFBP2–IGFII complex (APMA_IGFBP2–IGFII) conditions. Arrows show the increase in cell growth, which differed between the two experiment durations (see text for details) (B,C) MTT conversion was measured after either 3 or 6 days. The experiments were carried out in sextuples. All data are expressed in terms of means of absorbance ± SE. Only the significant differences (posthoc tests) are indicated as $*P < 0.05$, $**P < 0.01$, and $***P < 0.001$, with CT taken as reference in (A) and (B), and APMA_CT or APMA_IGFBP2–IGFII in (C).

about the IGF system and proteases may provide new targets for therapeutic approaches undertaken in the search for alternative treatment in human astrocytomas.

ACKNOWLEDGMENTS

REFERENCES

Andrews DW, Resnicoff M, Flanders AE, Kenyon L, Curtis M, Merli G, Baserga R, Iliakis G, Aiken RD. 2001. Results of a pilot study involving the use of an antisense oligodeoxynucleotide directed against the insulin-like growth factor type I receptor in malignant astrocytomas. J Clin Oncol 19:2189–2200.

Antoniades HN, Galanopoulos T, Neville-Golden J, Maxwell M. 1992. Expression of insulin-like growth factors I, II, their receptor mRNAs in primary human astrocytomas and meningiomas; in vivo studies using in situ hybridization and immunocytochemistry. Int J Cancer 50:215–222.

Arai K, Lee SR, Lo EH. 2003. Essential role for ERK mitogen-activated protein kinase in matrix metalloproteinase-9 regulation in rat cortical astrocytes. Glia 43:254–264.

Belien AT, Paganetti PA, Schwab ME. 1999. Membrane-type 1 matrix metalloprotease (MT1-MMP) enables invasive migration of glioma cells in central nervous system white matter. J Cell Biol 144:373–384.

Bellail AC, Hunter SB, Brat DJ, Tan C, Van Meir EG. 2004. Microregional extracellular matrix heterogeneity in brain modulates glioma cell invasion. Int J Biochem Cell Biol 36:1046–1069.

Brockmann MA, Ulbricht U, Gruner K, Fillbrandt R, Westphal M, Lamszus K. Glioblastoma and cerebral microvascular endothelial cell migration in response to tumor-associated growth factors. Neurosurgery 52:1391–9, 2003; discussion 1399.

Bunn RC, Fowlkes JL. 2003. Insulin-like growth factor binding protein proteolysis. Trends Endocrinol Metab 14:176–181.

Chesik D, De Keyser J, Wilczak N. 2007. Insulin-like growth factor binding protein-2 as a regulator of IGF actions in CNS: Implications in multiple sclerosis. Cytokine Growth Factor Rev 18(3/4):267–278.

Chesik D, Kuhl NM, Wilczak N, De Keyser J. 2004. Enhanced production and proteolytic degradation of insulin-like growth factor binding protein-2 in proliferating rat astrocytes. J Neurosci Res 77:354–362.

Chiappori AA, Eckhardt SG, Bukowski R, Sullivan DM, Ikeda M, Yano Y, Yamada-Sawada T, Kambayashi Y, Tanaka K, Javle MM, Mekhail T, O'bryant CL, Creaven PJ. 2007. A phase I pharmacokinetic and pharmacodynamic study of s-3304, a novel matrix metalloproteinase inhibitor, in patients with advanced and refractory solid tumors. Clin Cancer Res 13:2091–2099.

Claussen M, Kubler B, Wendland M, Neifer K, Schmidt B, Zapf J, Braulke T. 1997. Proteolysis of insulin-like growth factors (IGF) and IGF binding proteins by cathepsin D. Endocrinology 138:3797–3803.

Coppock HA, White A, Aplin JD, Westwood M. 2004. Matrix metalloprotease-3 and -9 proteolyze insulin-like growth factor-binding protein-1. Biol Reprod 71:438–443.

Crocker SJ, Pagenstecher A, Campbell IL. 2004. The TIMPs tango with MMPs and more in the central nervous system. J Neurosci Res 75:1–11.

Debeir O, Van Ham P, Kiss R, Decaestecker C. 2005. Tracking of migrating cells under phase-contrast video microscopy with combined mean-shift processes. IEEE Trans Med Imaging 24:697–711.

DeClerck YA, Mercurio AM, Stack MS, Chapman HA, Zutter MM, Muschel RJ, Raz A, Matrisian LM, Sloane BF, Noel A, Hendrix MJ, Coussens L, Padarathsingh M. 2004. Proteases, extracellular matrix, and cancer: A workshop of the path B study section. Am J Pathol 164:1131–1139.

Egeblad M, Werb Z. 2002. New functions for the matrix metalloproteinases in cancer progression. Nat Rev Cancer 2:161–174.

Firth SM, Baxter RC. 2002. Cellular actions of the insulin-like growth factor binding proteins. Endocr Rev 23:824–854.

Fowlkes JL, Enghild JJ, Suzuki K, Nagase H. 1994. Matrix metalloproteinases degrade insulin-like growth factor-binding protein-3 in dermal fibroblast cultures. J Biol Chem 269:25742–25746.

Friedl P, Hegerfeldt Y, Tusch M. 2004. Collective cell migration in morphogenesis and cancer. Int J Dev Biol 48(5/6):441–449.

Giese A, Bjerkvig R, Berens ME, Westphal M. 2003. Cost of migration: Invasion of malignant gliomas and implications for treatment. J Clin Oncol 21:1624–1636.

Groft LL, Muzik H, Rewcastle NB, Johnston RN, Knauper V, Lafleur MA, Forsyth PA, Edwards DR. 2001. Differential expression and localization of TIMP-1 and TIMP-4 in human gliomas. Br J Cancer 85:55–63.

Guvakova MA. 2007. Insulin-like growth factors control cell migration in health and disease. Int J Biochem Cell Biol 39:890–909.

Hoeflich A, Reisinger R, Lahm H, Kiess W, Blum WF, Kolb HJ, Weber MM, Wolf E. 2001. Insulin-like growth factor-binding protein 2 in tumorigenesis: Protector or promoter? Cancer Res 61:8601–8610.

Imai K, Hiramatsu A, Fukushima D, Pierschbacher MD, Okada Y. 1997. Degradation of decorin by matrix metalloproteinases: Identification of the cleavage sites, kinetic analyses and transforming growth factor-beta1 release. Biochem J 322 (Pt 3):809–814.

Kajita M, Itoh Y, Chiba T, Mori H, Okada A, Kinoh H, Seiki M. 2001. Membrane-type 1 matrix metalloproteinase cleaves CD44 and promotes cell migration. J Cell Biol 153:893–904.

Kleihues P, Cavenee WK. 2000. WHO classification of tumours. Pathology and genetics of tumours of the nervous system. Lyon: IARC Press.

Lakka SS, Gondi CS, Dinh DH, Olivero WC, Gujrati M, Rao VH, Sioka C, Rao JS. 2005. Specific interference of urokinase-type plasminogen activator receptor and matrix metalloproteinase-9 gene expression induced by double-stranded RNA results in decreased invasion, tumor growth, and angiogenesis in gliomas. J Biol Chem 280:21882–21892.

Lakka SS, Rajan M, Gondi C, Yanamandra N, Chandrasekar N, Jasti SL, Adachi Y, Siddique K, Gujrati M, Olivero W, Dinh DH, Kouraklis G, Kyritsis AP, Rao JS. 2002. Adenovirus-mediated expression of antisense MMP-9 in glioma cells inhibits tumor growth and invasion. Oncogene 21:8011–8019.

Lampert K, Machein U, Machein MR, Conca W, Peter HH, Volk B. 1998. Expression of matrix metalloproteinases and their tissue inhibitors in human brain tumors. Am J Pathol 153:429–437.

Levitt RJ, Georgescu MM, Pollak M. 2005. PTEN-induction in U251 glioma cells decreases the expression of insulin-like growth factor binding protein-2. Biochem Biophys Res Commun 336:1056–1061.

Manes S, Llorente M, Lacalle RA, Gomez-Mouton C, Kremer L, Mira E, Martinez AC. 1999. The matrix metalloproteinase-9 regulates the insulin-like growth factor-triggered autocrine response in DU-145 carcinoma cells. J Biol Chem 274:6935–6945.

Manes S, Mira E, Barbacid MM, Cipres A, Fernandez-Resa P, Buesa JM, Merida I, Aracil M, Marquez G, Martinez AC. 1997. Identification of insulin-like growth factor-binding protein-1 as a potential physiological substrate for human stromelysin-3. J Biol Chem 272:25706–25712.

McCawley LJ, Matrisian LM. 2001. Matrix metalloproteinases: They're not just for matrix anymore! Curr Opin Cell Biol 13:534–540.

Menouny M, Binoux M, Babajko S. 1997. Role of insulin-like growth factor binding protein-2 and its limited proteolysis in neuroblastoma cell proliferation: Modulation by transforming growth factor-beta and retinoic acid. Endocrinology 138:683–690.

Miyamoto S, Yano K, Sugimoto S, Ishii G, Hasebe T, Endoh Y, Kodama K, Goya M, Chiba T, Ochiai A. 2004. Matrix metalloproteinase-7 facilitates insulin-like growth factor bioavailability through its proteinase activity on insulin-like growth factor binding protein 3. Cancer Res 64:665–671.

Morford LA, Boghaert ER, Brooks WH, Roszman TL. 1997. Insulin-like growth factors (IGF) enhance three-dimensional (3D) growth of human glioblastomas. Cancer Lett 115:81–90.

Nakamura M, Miyamoto S, Maeda H, Ishii G, Hasebe T, Chiba T, Asaka M, Ochiai A. 2005. Matrix metalloproteinase-7 degrades all insulin-like growth factor binding proteins and facilitates insulin-like growth factor bioavailability. Biochem Biophys Res Commun 333:1011–1016.

Nakano A, Tani E, Miyazaki K, Yamamoto Y, Furuyama J. 1995. Matrix metalloproteinases and tissue inhibitors of metalloproteinases in human gliomas. J Neurosurg 83:298–307.

Nuttall RK, Pennington CJ, Taplin J, Wheal A, Yong VW, Forsyth PA, Edwards DR. 2003. Elevated membrane-type matrix metalloproteinases in gliomas revealed by profiling proteases and inhibitors in human cancer cells. Mol Cancer Res 1:333–345.

Palermo C, Manduca P, Gazzerro E, Foppiani L, Segat D, Barreca A. 2004. Potentiating role of IGFBP-2 on IGF-II-stimulated alkaline phosphatase activity in differentiating osteoblasts. Am J Physiol Endocrinol Metab 286:E648–E657.

Rajaram S, Baylink DJ, Mohan S. 1997. Insulin-like growth factor-binding proteins in serum and other biological fluids: Regulation and functions. Endocr Rev 18:801–831.

Rao JS. 2003. Molecular mechanisms of glioma invasiveness: The role of proteases. Nat Rev Cancer 3:489–501.

Rao JS, Bhoopathi P, Chetty C, Gujrati M, Lakka SS. 2007. MMP-9 short interfering RNA induced senescence resulting in inhibition of medulloblastoma growth via p16(INK4a) and mitogen-activated protein kinase pathway. Cancer Res 67:4956–4964.

Rorive S, Belot N, Decaestecker C, Lefranc F, Gordower L, Micik S, Maurage CA, Kaltner H, Ruchoux MM, Danguy A, Gabius HJ, Salmon I, Kiss R, Camby I. 2001. Galectin-1 is highly expressed in human gliomas with relevance for modulation of invasion of tumor astrocytes into the brain parenchyma. Glia 33:241–255.

Rorive S, Maris C, Debeir O, Sandras F, Vidaud M, Bieche I, Salmon I, Decaestecker C. 2006. Exploring the distinctive biological characteristics of pilocytic and low-grade diffuse astrocytomas using microarray gene expression profiles. J Neuropathol Exp Neurol 65:794–807.

Baserga R, Prisco M, Hongo A. 1999. IGFs and cell growth. In: Rosenfeld RG, Roberts CT Jr, editors. The IGF system: Molecular biology, physiology, and clinical applications. Totowa, New Jersey: Humana Press. pp 329–353.

Leventhal PS, Russell JW, Feldman EL. 1999. IGFs and the nervous system. In: Rosenfeld RG, Roberts CT Jr, editors. The IGF system: Molecular biology, physiology, and clinical applications. Totowa, New Jersey: Humana Press. pp 425–455.

Sallinen SL, Sallinen PK, Haapasalo HK, Helin HJ, Helen PT, Schraml P, Kallioniemi OP, Kononen J. 2000. Identification of differentially expressed genes in human gliomas by DNA microarray and tissue chip techniques. Cancer Res 60:6617–6622.

Soroceanu L, Kharbanda S, Chen R, Soriano RH, Aldape K, Misra A, Zha J, Forrest WF, Nigro JM, Modrusan Z, others. 2007. Identification of IGF2 signaling through phosphoinositide-3-kinase regulatory subunit 3 as a growth-promoting axis in glioblastoma. Proc Natl Acad Sci USA 104:3466–3471.

Thrailkill KM, Quarles LD, Nagase H, Suzuki K, Serra DM, Fowlkes JL. 1995. Characterization of insulin-like growth factor-binding protein 5-degrading proteases produced throughout murine osteoblast differentiation. Endocrinology 136:3527–3533.

Tong AW, Zhang YA, Nemunaitis J. 2005. Small interfering RNA for experimental cancer therapy. Curr Opin Mol Ther 7:114–124.

Toretsky JA, Helman LJ. 1996. Involvement of IGF-II in human cancer. J Endocrinol 149:367–372.

Trojan J, Cloix JF, Ardourel MY, Chatel M, Anthony DD. 2007. Insulin-like growth factor type I biology and targeting in malignant gliomas. Neuroscience 145:795–811.

Visse R, Nagase H. 2003. Matrix metalloproteinases and tissue inhibitors of metalloproteinases: Structure, function, and biochemistry. Circ Res 92:827–839.

Wang GK, Hu L, Fuller GN, Zhang W. 2006. An interaction between insulin-like growth factor-binding protein 2 (IGFBP2) and integrin alpha5 is essential for IGFBP2-induced cell mobility. J Biol Chem 281:14085–14091.

Wang H, Wang H, Shen W, Huang H, Hu L, Ramdas L, Zhou YH, Liao WS, Fuller GN, Zhang W. 2003. Insulin-like growth factor binding protein 2 enhances glioblastoma invasion by activating invasion-enhancing genes. Cancer Res 63:4315–4321.

Woo MS, Jung SH, Kim SY, Hyun JW, Ko KH, Kim WK, Kim HS. 2005. Curcumin suppresses phorbol ester-induced matrix metalloproteinase-9 expression by inhibiting the PKC to MAPK signaling pathways in human astroglioma cells. Biochem Biophys Res Commun 335:1017–1025.

Yan L, Borregaard N, Kjeldsen L, Moses MA. 2001. The high molecular weight urinary matrix metalloproteinase (MMP) activity is a complex of gelatinase B/MMP-9 and neutrophil gelatinase-associated lipocalin (NGAL). Modulation of MMP-9 activity by NGAL. J Biol Chem 276:37258–37265.

Yu Q, Stamenkovic I. 2000. Cell surface-localized matrix metalloproteinase-9 proteolytically activates TGF-beta and promotes tumor invasion and angiogenesis. Genes Dev 14:163–176.

Zeger M, Popken G, Zhang J, Xuan S, Lu QR, Schwab MH, Nave KA, Rowitch D, D'Ercole AJ, Ye P. 2007. Insulin-like growth factor type 1 receptor signaling in the cells of oligodendrocyte lineage is required for normal in vivo oligodendrocyte development and myelination. Glia 55:400–411.